Binding of camphor to *Pseudomonas putida* cytochrome P450$_{cam}$: steady-state and picosecond time-resolved fluorescence studies

Swati Prasad, Shyamalava Mazumdar, Samaresh Mitra*

Department of Chemical Sciences, Tata Institute of Fundamental Research, Homi Bhabha Road, Colaba, Mumbai 400005, India

Abstract **The binding of camphor to cytochrome P450$_{cam}$ has been investigated by steady-state and time-resolved tryptophan fluorescence spectroscopy to obtain information on the substrate access channel. The fluorescence quenching experiments show that some of the tryptophan residues undergo changes in their local environment on camphor binding. The time-resolved fluorescence decay profile gives four lifetime components in the range from 99 ps to 4.5 ns. The shortest lifetime component assigned to W42 lies close to the proposed camphor access channel. The results show that the fluorescence of W42 is greatly affected on binding of camphor, and supports dynamic fluctuations involved in the passage of camphor through the access channel as proposed earlier on the basis of crystallographic, molecular dynamics simulation and site-directed mutagenesis studies. © 2000 Federation of European Biochemical Societies. Published by Elsevier Science B.V. All rights reserved.**

Key words: Cytochrome P450$_{cam}$; Substrate binding; Substrate access channel; Steady-state fluorescence; Picosecond time-resolved fluorescence; Conformational change

1. Introduction

Cytochrome P450 enzymes are hemeprotein monooxygenases that catalyze the oxidation of a variety of hydrophobic compounds of xenobiotic and endogenous origin [1,2]. Cytochrome P450$_{cam}$ (P450$_{cam}$) is a 45 kDa polypeptide chain containing a single ferric protoporphyrin IX, which catalyzes the stereospecific hydroxylation of camphor to 5-exo-hydroxycamphor at the expense of 1 mol each of NADH and dioxygen [3]. The first step in the catalytic cycle of P450$_{cam}$ involves binding of camphor, which is associated with the expulsion of the water molecule coordinated at the sixth position of the heme iron and a consequent change in the heme spin state from low spin to high spin [4]. Such a change in the axial ligation and spin state brings about changes in the conformation of the enzyme, which triggers its interaction with the redox partners [5].

Hydroxylation of camphor by P450$_{cam}$ involves transfer of an oxygen atom to it through the redox catalytic cycle of the heme active site. The substrate binding site lies in close proximity of the heme moiety. The X-ray crystal structures of camphor-free [6] and camphor-bound [7] P450$_{cam}$ have been reported (Fig. 1), which show that the heme moiety in P450$_{cam}$ is buried ∼20 Å deep inside the enzyme, isolated from the solvent. There is considerable interest in the camphor access channel for the entry of the substrate into the active site of P450$_{cam}$. Poulos et al. [6,7] have addressed this problem and have observed that the crystal structures of P450$_{cam}$ do not define an open cleft at the molecular surface for the entry of substrate into the active site region of P450$_{cam}$. A small opening at the molecular surface near the active site was proposed but it was considered to be too small to accommodate camphor. Poulos et al. [6,7] have further suggested that the camphor access channel in P450$_{cam}$ undergoes dynamic fluctuations to enable the camphor molecule to enter the active site. Molecular dynamics simulation studies based on the thermal motion pathway analysis [8,9] have indicated that the camphor access channel in P450$_{cam}$ is lined by aromatic residues (Y96, F87, Y29 and F193) and involves motion of the flexible F-G helix-loop-helix segment of the enzyme (Fig. 1). Three regions, namely, the helix B′, the loop joining helices F and G and the salt bridge Asp-251–Arg-186, have been implicated for the access of the substrate to the active site on the basis of crystallographic, molecular dynamics simulation and site-directed mutagenesis studies [8–11].

The structural data show that P450$_{cam}$ has five tryptophan residues (W42, W55, W63, W374 and W406), among which W42 is nearest to the proposed camphor access channel (Fig. 1). The intrinsic fluorescence of the indole moiety of tryptophan residue is very sensitive to its environment and has been extensively used to probe conformational/dynamical changes in proteins [12]. Any structural or dynamic fluctuations involved in the passage of the substrate through the access channel would affect W42 because of its vicinity to the proposed camphor access channel. Thus, the fluorescence properties of W42 residue in absence and presence of the substrate can provide information on the structural fluctuations involving entry/passage of the substrate through the proposed access channel. These considerations have led us to carry out steady-state and time-resolved tryptophan fluorescence studies on the camphor-free and camphor-bound P450$_{cam}$. Our studies support dynamic fluctuations in the helix B′ region and opening of the camphor access channel next to the F-G loop on binding of camphor, as proposed earlier [6,7].

2. Materials and methods

2.1. Materials

DEAE Sepharose, Q Sepharose, Sephadex G10 column, *N*-acetyltryptophanamide (NATA) and acrylamide were purchased from Sigma. Potassium iodide (KI) was obtained from E. Merck. All other chemicals were of analytical grade.

2.2. Protein purification

Pseudomonas putida P450$_{cam}$ was overexpressed in *Escherichia coli*

*Corresponding author. Fax: (91)-22-2152110.
E-mail: smitra@tifr.res.in

and purified according to the reported method [13]. The enzyme preparation was stored at −20°C in 1 mM camphor and 40 mM phosphate, pH 7.4, solution containing 50% glycerol.

2.3. Steady-state fluorescence spectroscopy

Steady-state fluorescence measurements were done on a Spex Fluorolog-1681T spectrofluorometer. The fluorescence excitation wavelength was kept at 295 nm and the measured fluorescence intensity (F_{obs}) after the addition of a quencher was corrected for the enzyme dilution and inner filter effect as described earlier [12]. The tryptophan fluorescence quenching experiments were performed using acrylamide (neutral quencher) and KI (ionic quencher) as described earlier [14,15].

2.4. Time-resolved fluorescence spectroscopy

The time-resolved tryptophan fluorescence studies were carried out with a synchronously pumped cavity-dumped mode-locked picosecond dye laser (Rhodamine 6G) set up, equipped with time-correlated single photon counting device described elsewhere [16]. Width of the dye laser pulse was typically 4 ps and the half-width of the instrument response function was typically about 100 ps. The tunable output of dye laser was frequency-doubled to generate the ultraviolet beam at 295 nm, which was used to excite the samples. Emission profiles were collected at the magic angle (54.7°) of emission polarizer to avoid any contribution from anisotropy. Protein samples (5 μM) in 40 mM potassium phosphate buffer pH 7.4 were used for the time-resolved fluorescence measurements.

Fluorescence decay curves were deconvoluted with the excitation function and the fluorescence intensities were analyzed. The amplitudes and lifetimes were determined by applying an iterative reconvolution using non-linear least square regression by Marquardt's algorithm for parameter optimization [17]. Analysis of the fluorescence decay profiles was also carried out by the maximum entropy method (MEM) using 150 lifetime components ranging from 0.01 to 10 ns uniformly distributed in a logarithmic time scale [18,19].

The decay-associated emission spectra (DAS) of tryptophan fluorescence were computed from the steady-state spectra and the time-resolved fluorescence decay parameters $\alpha_i(\lambda)$ and $\tau_i(\lambda)$ at emission wavelengths ranging from 310 to 375 nm [20,21].

2.5. Fluorescence energy transfer

The tryptophan fluorescence of the hemeproteins is dominated by fast decay kinetics with lifetime components in the subnanosecond range [22]. The efficiency of energy transfer (E) depends on the distance (R) and the relative orientation of heme and tryptophan residues [12,22], and is related by the Eq. 1:

$$E = \frac{R_o^6}{R^6 + R_o^6} = 1 - \frac{\tau_{da}}{\tau_d} \qquad (1)$$

where, τ_{da} and τ_d represent the lifetime of tryptophan in presence and in absence of heme, respectively. R_o is the distance for 50% energy transfer efficiency. R_o was calculated using the following relation:

$$R_o = (J\kappa^2 Q_d n^{-4})^{1/6} \times 9.79 \times 10^3 \text{ Å} \qquad (2)$$

where J is the spectral overlap integral of the normalized emission spectrum of the donor tryptophans and absorption spectrum of the acceptor heme. The value of overlap integral was found to be 3.7×10^{-14} cm^3 M^{-1}, as calculated by the reported method [23,24]. n ($n = 1.4$) is the refractive index of the medium. Q_d is the quantum yield of tryptophan ($Q_d = 0.13$) in absence of any quencher [14]. κ^2 is the orientation factor of the tryptophan–heme transition moments and is defined by the direction of the transition moment of the donor (tryptophan) and acceptor (heme). κ^2 can be computed for the hemeproteins using their atomic coordinates, and the experimentally observed lifetimes can be correlated to the structural disposition of their tryptophan residues [25].

3. Results and discussion

The fluorescence emission spectrum of P450$_{cam}$ shows a broad peak at 325 nm indicating relatively non-polar average environment around the five tryptophan residues of P450$_{cam}$ with a dielectric constant similar to *p*-dioxane and butyl ether
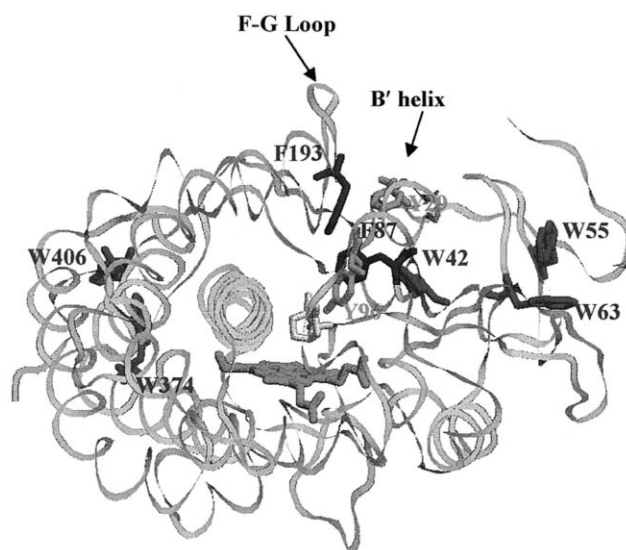

Fig. 1. Schematic structure of camphor-bound cytochrome P450$_{cam}$.

[26]. The addition of camphor to the camphor-free P450$_{cam}$ causes very little change in its peak position though its fluorescence intensity decreases by 1.6 times. This decrease in fluorescence intensity may be attributed to the increase in the overlap integral, due to blue shift of the Soret band (from 417 nm to 392 nm) on binding of camphor to camphor-free P450$_{cam}$. The relative quantum yields for camphor-bound and camphor-free P450$_{cam}$ measured using NATA as reference were found to be similar (0.019 ± 0.001). The fluorescence quantum yields for tryptophan in hemeproteins are generally low [27] as compared to their apo proteins, due to efficient energy transfer from tryptophan residues to the heme.

The tryptophan fluorescence quenching experiments with acrylamide and KI were done to determine surface accessibility of the tryptophan residues of P450$_{cam}$ and its complex with camphor. Acrylamide is a hydrophobic and neutral quencher, whereas KI is an ionic quencher. Fig. 2A shows that Stern–Volmer plot of acrylamide quenching is linear for both camphor-free and camphor-bound enzyme, indicating that all the five tryptophan residues are accessible to acrylamide. The plot for KI with both camphor-free and camphor-bound enzyme shows downward curvature at higher concentration of KI (Fig. 2A). KI being an ionic quencher cannot penetrate into the hydrophobic core of the protein. The percentage of the total fluorescence quenched by KI was found to be $17 \pm 1\%$ as only part of the tryptophan fluorescence is quenched. The fraction of tryptophan accessible to ionic quencher (KI) was calculated from a Lehrer plot (Fig. 2B) [14,15], and found to be 0.16 and 0.28 for camphor-free and camphor-bound P450$_{cam}$, respectively. This suggests that on binding of camphor some of the tryptophan residues become accessible to the quencher due to changes in their local environment. The Stern–Volmer quenching constant (K_{sv}) with acrylamide was found to be larger for camphor-free P450$_{cam}$ (1.45 M^{-1}) than for camphor-bound P450$_{cam}$ (0.72 M^{-1}), indicating greater fluctuations in the camphor-free enzyme, which facilitates diffusion of acrylamide inside the enzyme [28]. The large decrease in K_{sv} upon binding of camphor to P450$_{cam}$ may arise due to decrease in local dynamic fluctuations of camphor entry channel owing to specific protein–substrate interactions
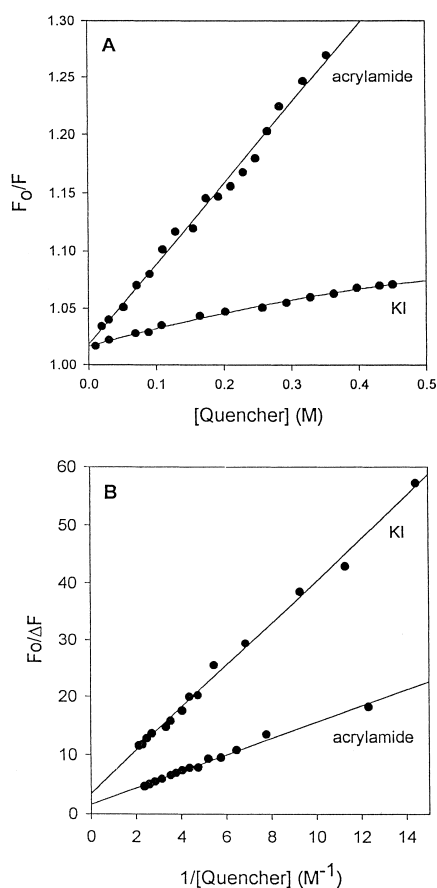
Fig. 3. Time-resolved fluorescence decay of camphor-bound cytochrome $P450_{cam}$ (a) and the instrument response function (b). The solid line through the decay curve shows the four exponential fit. The upper curve in the figure shows the weighted residual $[F_{cal}(t)-F_{exp}(t)]$ plot illustrating the accuracy of the exponential fit.

Fig. 2. (A) Stern–Volmer plots for tryptophan fluorescence quenching of camphor-bound cytochrome $P450_{cam}$ by acrylamide and KI. (B) Lehrer plot for tryptophan fluorescence quenching of camphor-bound cytochrome $P450_{cam}$ by acrylamide and KI. The Stern–Volmer and Lehrer plots for camphor-free cytochrome $P450_{cam}$ are not shown.

[6], and/or from the decrease in fluorescence quenching of W42 lying in the vicinity of proposed substrate entry channel.

Fig. 3 shows a typical time-resolved fluorescence decay profile of the camphor-bound cytochrome $P450_{cam}$. The fluorescence decay curves for both camphor-free and camphor-bound $P450_{cam}$ were best fitted to a sum of four exponentials, as judged by random residuals distribution, autocorrelation function and χ^2 minimization criteria. The fluorescence lifetimes (their amplitude in parentheses) obtained for the camphor-bound enzyme were $\tau_1 = 0.099$ (55%), $\tau_2 = 0.27$ (42%), $\tau_3 = 1.18$ (2%), $\tau_4 = 4.49$ ns (1%) and those for the camphor-free enzyme were $\tau_1 = 0.126$ (57%), $\tau_2 = 0.29$ (40%), $\tau_3 = 1.23$ (2%), $\tau_4 = 4.47$ ns (1%), respectively. The two faster lifetime components (τ_1 and τ_2) account for almost 97% of the observed fluorescence. The longest lifetime component (τ_4) may be due to presence of non-heme impurities [29]. The binding of camphor to camphor-free $P450_{cam}$ thus greatly affects the shortest lifetime component (τ_1) and decreases it by 27% (from 0.126 to 0.099 ns), whereas the other lifetime components are not significantly affected.

The validity of the four exponential model to analyze the fluorescence decay data was further checked using MEM [18,19]. The MEM simulation for both camphor-free and camphor-bound enzyme was found to give similar lifetime distributions, with bericenters of four distinct classes around
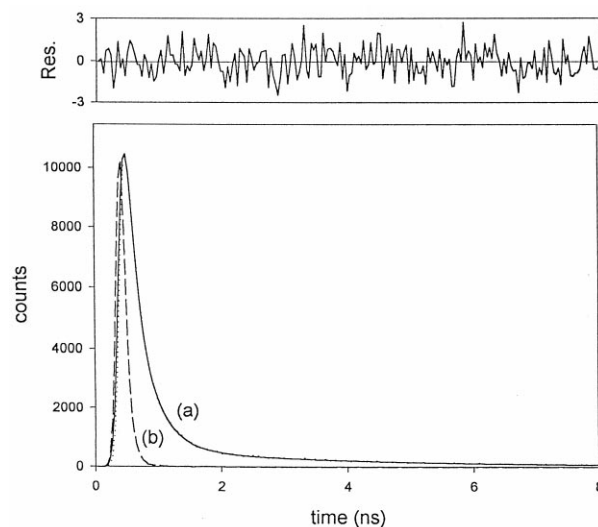
0.1, 0.3, 1.7 and 4.8 ns (data not shown). These values are almost identical to the lifetimes obtained by the discrete analysis method.

The bimolecular rate constant for acrylamide quenching of camphor-free and camphor-bound $P450_{cam}$ was calculated using K_{sv} and the average lifetimes of the tryptophans in both camphor-free and camphor-bound $P450_{cam}$. These rate constants were found to be 5.5×10^9 and 2.7×10^9 M^{-1} s^{-1} for camphor-free and camphor-bound $P450_{cam}$, respectively. Such a high bimolecular rate constant for $P450_{cam}$ supports dynamic fluctuation in the enzyme as quenching of tryptophan fluorescence by acrylamide would require penetration of acrylamide through channels in the protein matrix.

The DAS of the individual lifetime components of the camphor-bound and camphor-free enzyme are almost identical. The fluorescence emission maxima are known to be dependent on the hydrophobicity of tryptophan environment [12]. The
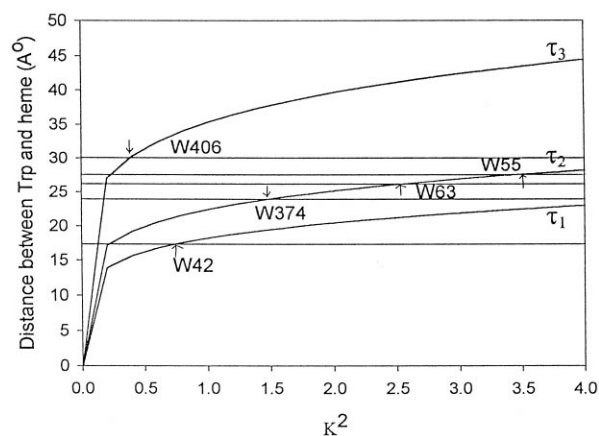

Fig. 4. Variation of distance of different tryptophans from heme with κ^2 (orientation factor). The point where the heme–tryptophan crystallographic distance (horizontal line) and calculated distance (lines labeled τ_1, τ_2 and τ_3) intersect shows the κ^2 value for the particular residue and is indicated by arrows.

emission maxima for individual lifetime components $\lambda(\tau_i)$ were found to be $\lambda(\tau_1) = 320$, $\lambda(\tau_2) = 327$, $\lambda(\tau_3) = 330$ and $\lambda(\tau_4) = 340$ nm. This indicates that the shortest lifetime component (τ_1) originates from tryptophan that is buried in the core of the enzyme and is not accessible to the solvent, while other lifetime components may originate from tryptophan residues that are completely or partially accessible to the solvent.

The position and orientation of the tryptophan residues with respect to heme were correlated to experimentally observed individual lifetime components using Eqs. 1 and 2). The relative orientation of heme and tryptophan chromophores is expressed through the orientation factor κ^2 (see Section 2). Fig. 4 shows variation of the tryptophan–heme energy transfer distance with the orientation factor κ^2. The horizontal lines in the plot represent the crystallographic distances of the five tryptophans from heme (W42: 17.3 AÅ, W55: 27.6 Å, W63: 26.2 Å, W374: 24 Å and W406: 30.1 Å), as determined from the atomic coordinates of P450$_{cam}$ [7] (using the program Biosym MSI Inc.). The distances between heme and different tryptophan residues (labeled τ_1, τ_2 and τ_3) were calculated using Eqs. 1 and 2) for possible values of κ^2. The values of κ^2 vary from 0 to 4 depending on the relative orientation of tryptophan and heme. The extreme values of $\kappa^2 = 0$ and $\kappa^2 = 4$ represent perpendicular and parallel orientation of heme and tryptophan dipoles with respect to one another, respectively. The line labeled τ_1 intersects the horizontal line corresponding to W42 at a value of $\kappa^2 \sim 0.8$, which is in agreement with the crystallographic data [7]. Therefore, the shortest lifetime component (τ_1) is assigned to W42. W42 is buried in the core of the enzyme and is closest to the substrate access channel. Our results show that its fluorescence is greatly affected by the binding of camphor and provide experimental support to the dynamic fluctuations involved in the entry/passage of camphor through the proposed camphor access channel next to the flexible F-G helix-loop-helix segment. The other lifetime components may be assigned to the remaining four tryptophan residues (W55, 63, 374 and 406). However, unlike W42, the assignment of the lifetimes of these tryptophan residues may not be unambiguous. Moreover, the fluorescence of these four tryptophan residues does not change significantly upon binding of camphor because the segments of enzyme containing them are far removed from the substrate access channel.

References

[1] Guengerich, F.P. (1991) J. Biol. Chem. 266, 10019–10022.
[2] Porter, T.D. and Coon, M.J. (1991) J. Biol. Chem. 266, 13469–13472.
[3] Katagiri, M., Ganguli, B.N. and Gunsalus, I.C. (1968) J. Biol. Chem. 243, 3543–3546.
[4] White, R.E. and Coon, M.J. (1980) Annu. Rev. Biochem. 49, 315–356.
[5] Shiro, Y., Iizuka, T., Makino, R., Ishimura, Y. and Morishima, I. (1989) J. Am. Chem. Soc. 111, 7707–7711.
[6] Poulos, T.L., Finzel, B.C. and Howard, A.J. (1986) Biochemistry 25, 5314–5322.
[7] Poulos, T.L., Finzel, B.C. and Howard, A.J. (1987) J. Mol. Biol. 195, 687–700.
[8] Luedemann, S.K., Carugo, O. and Wade, R.C. (1997) J. Mol. Model. 3, 369–374.
[9] Wade, R.C., Gaboulline, R.R. and Ludemann, S.K. (1998) Proc. Natl. Acad. Sci. USA 95, 5942–5949.
[10] Mueller, E.J., Loida P.J. and Sligar, S.G. (1995) in: Cytochrome P450: Structure, Mechanism, and Biochemistry (Ortis de Montellano, P.R., Ed.), 2nd edn., pp. 83–124, Plenum Press, New York.
[11] Raag, R., Li, H. and Jones, B.C. (1993) Biochemistry 32, 4571–4578.
[12] Lakowicz, J.R. (1983) Principles of Fluorescence Spectroscopy, Plenum Press, New York.
[13] Unger, B.P. and Gunsalus, I.C. (1986) J. Biol. Chem. 261, 1158–1163.
[14] Lehrer, S.S. (1971) Biochemistry 10, 3254–3263.
[15] Khan, K.K., Mazumdar, S., Modi, S., Sutcliffe, M., Roberts, G.C.K. and Mitra, S. (1997) Eur. J. Biochem. 244, 361–370.
[16] Periaswamy, N., Doraiswamy, S., Maiya, G.B. and Venkataraman, B. (1988) J.Chem. Phys. 88, 1638–1651.
[17] Bevington, P.R. (1969) Data Reduction and Error Analysis for the Physical Sciences, McGraw-Hill Inc., New York.
[18] Livesey, A.K. and Brochon, A.K. (1987) Biophys. J. 52, 693–706.
[19] Vincent, M., Brochon, J.C., Merola, F. and Jordi, W. (1988) Biochemistry 27, 8752–8761.
[20] Robbins, D.J., Deibel Jr., M.R. and Barkley, M.D. (1985) Biochemistry 24, 7250–7257.
[21] Yip, R.W., Wen, Y.-X. and Szabo, A.G. (1993) J. Phys. Chem. 97, 10458–10462.
[22] Hochstrasser, R.M. and Negus, D.K. (1984) Proc. Natl. Acad. Sci. USA 81, 4399–4403.
[23] Cheung, H.C. (1992) Topics in Fluorescence Spectroscopy (Lakowicz, J.R, Ed.), Vol. 2, pp. 128–176, Plenum Press, New York.
[24] Campbell, I.D. and Dwek, R.A. (1984) Biological Spectroscopy, Benjamin Cummings, Menlo Park.
[25] Gryczynski, Z., Lubkowski, J. and Bucci, E. (1997) Methods Enzymol. 278, 538–569.
[26] Cowgill, R.W. (1967) Biochim. Biophys. Acta 133, 6–18.
[27] Weber, G. (1959) Discuss. Faraday Soc. 27, 134–141.
[28] Eftnik, M.K. and Ghiron, C.A. (1981) Anal. Biochem. 114, 199–227.
[29] Beechem, J.M. and Brand, L. (1985) Annu. Rev. Biochem. 54, 43–71.